RNA (1995), *1*:538-550. Cambridge University Press. Printed in the USA.

Selection of an RNA domain that binds Zn^{2+}

JERZY CIESIOLKA, JESSICA GORSKI, and MICHAEL YARUS
Department of MCD Biology, University of Colorado, Boulder, Colorado 80309-0347, USA

ABSTRACT

We have selected an RNA that depends on zinc for affinity to a column, starting from a pool of ribooligonucleotides with 50 randomized positions. This RNA's chemical sensitivities, calculated folding thermodynamics, and activity when fragmented suggest that an ion binding site lies within a complex 21-nt hairpin loop, near the junction with an imperfect helical stem. This RNA site has an unselected selectivity among divalents, preferring nickel, cobalt, and cadmium to calcium, magnesium, and manganese, as expected for a simple site of chelation. A moderate zinc-dependent change in loop structure accompanies divalent binding and can be detected by chemical probing and zinc-dependent UV-induced crosslinking. The latter also demonstrates the apposition of loop sequences to make a structure that may be related to the E-loop motif found in a number of other RNA molecules; the E-loop motif, accordingly, may be a divalent site.

Keywords: divalent ion–RNA interactions; IMAC; metal ion affinity chromatography; RNA structure; selection–amplification; SELEX

INTRODUCTION

Metal ions are indispensable components of all biological systems. In many protein enzymes, metal ions not only play a structural role, but actively participate in catalytic processes (Walsh, 1977; Fersht, 1985). More recently it has been realized that metal ions may play a similar dual role in nucleic acids, crucial for catalysis by ribozymes in particular. Thus, in all characterized ribozymes, divalent metal ions are required not only for the formation of active structures, but also may participate directly in catalysis (for review see Pan et al., 1993; Yarus, 1993). Thus, it is likely that information about RNA-divalent binding sites will help understand RNA catalysis.

Information concerning metal coordination in RNA is still very limited; there are few proven generalizations concerning general principles that govern the interactions of structured, folded RNA molecules with divalent metal ions. Most information available so far derives from a few sites in solved tRNA crystal structures (reviewed in Teeter et al., 1980; Pan et al., 1993). The recent crystal structure of a hammerhead RNA–DNA ribozyme–inhibitor complex has significantly augmented this information; a small hammerhead RNA motif GAR/AG was proposed as a divalent ion-binding site (Pley et al., 1994).

Recently a new technique, selection–amplification, has allowed open-ended investigation of the fundamental capabilities of RNA (Ellington & Szostak, 1990; Tuerk & Gold, 1990). The power of that approach has been used for identifying in random RNA pools RNA motifs that bind varied small-molecular-weight ligand organic dye molecules (Ellington & Szostak, 1990), derivatized amino acids (Famulok & Szostak, 1992), free amino acids (Connell et al., 1993; Connell & Yarus, 1994; Famulok, 1994; Majerfeld & Yarus, 1994), ATP (Sassanfar & Szostak, 1993), GDP (Connell & Yarus, 1994), antibiotics (Davies et al., 1993), the alkaloid theophylline (Jenison et al., 1994), cyanocobalamin (Lorsch & Szostak, 1994), and the transition-state analog of a bridged biphenyl (Prudent et al., 1994). We have now exploited the method for selection of RNA molecules that bind Zn ions. This is the first elemental ion, and the smallest ligand, yet used in RNA selection–amplification experiments.

Our selection required affinity for chelated, but partially coordinated Zn^{2+}. Thus, a selected RNA, which is unlikely to bind all Zn^{2+} coordination positions, might be expected to allow other small molecules to gain access to the inner coordination sphere of its bound ion. Such accessible RNA-bound divalents might be useful in constructing new metallo-RNA catalysts (Yarus, 1993).

Reprint requests to: Michael Yarus, Department of MCD Biology, University of Colorado, Boulder, Colorado 80309-0347, USA; e-mail: yarus@beagle.colorado.edu.

RESULTS

Selection

As a selection procedure, we have used metal ion affinity chromatography on a column carrying iminodiacetic acid groups (IDA) charged with Zn ions (Fig. 1A). In the first round of selection, 20 μg of an RNA pool with a 50-nt randomized region was applied to the column (4×10^{14} molecules transcribed from 5×10^{13} different DNA templates). Following a wash to elute unbound or weakly bound molecules, only 0.03% of RNA was recovered by stripping the column of bound RNA and Zn ions with a buffer containing 50 mM EDTA. The EDTA-eluted RNA was desalted, reverse transcribed, amplified, transcribed with T7 RNA polymerase, and the enriched RNA pool used for the next round of selection. The heterogeneity of the RNA pools from each round was assayed by limited hydrolysis of these internally labeled RNAs using RNase T1 (Fig. 2). Uniformly distributed bands in the lanes corresponding to first four rounds turned to a distinct pattern after the fifth round of selection, indicating that the original pool with G's equally frequent at every position was being superseded by a selected group of specific sequences. This coincided with a jump in the amount of RNA recovered in the EDTA-fraction from 0.07 to 13.8% (Fig. 1A). Two additional rounds increased the amount of RNA bound to the column to more than 70%, but did not change the pattern of T1 RNase products. This pool's cDNAs were cloned and individual members were sequenced.

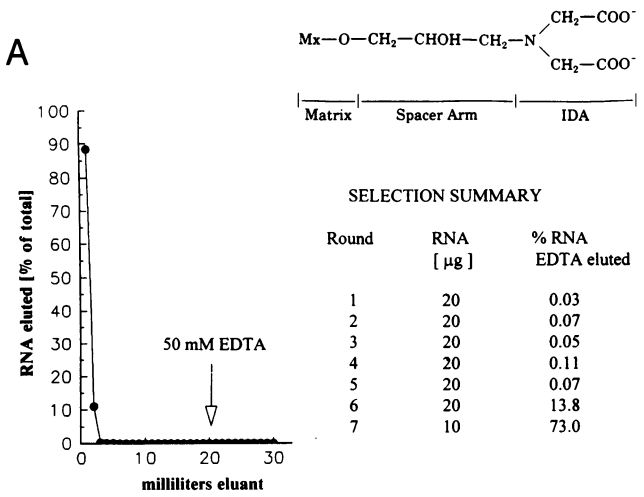

FIGURE 1. Selection of Zn-binding RNA by immobilized metal ion affinity chromatography on IDA-Sepharose column. **A:** Elution profile for round #1 and the selection summary. Internally ^{32}P-labeled RNA was loaded onto the Zn-column. After washing the column for 20 column volumes, any remaining RNA, as well as Zn ions, was eluted with 50 mM EDTA in the chromatography buffer. In the inset, the structure of the affinity matrix is shown. **B:** Elution profile for the selected, Zn-binding RNA.

The pool was virtually homogeneous: of 36 independent sequences, 30 were identical, 4 clones were related to the predominant sequence by point mutations, and 2 were unrelated to the major sequence as well as to each other. The RNAs from the latter unrelated clones were unable to bind to the Zn-column.

Binding of the selected RNA sequence to the IDA-column was strictly dependent on column-bound Zn ions. RNA applied to a column charged with Mg ions was eluted in the void volume ($K_d > 80$ mM), whereas 85% of applied RNA was eluted slowly from the Zn-charged column, 15% flowing through in the void volume (this fraction might represent misfolded molecules). Less than 4% was retained more strongly, but elutable with EDTA (Fig. 1B). The dissociation constant of the major peak was determined by isocratic ligand elution (Dunn & Chaiken, 1974; Connell et al., 1993) and found to be 1.2 ± 0.4 mM (Fig. 3). This isocratic elution with free Zn^{2+} also demonstrates that the RNA's sites for free and bound ion overlap, or are linked.

Structure of the selected RNA

A secondary structure for the Zn-binding RNA predicted by Mfold (Zuker, 1989) is shown in Figure 4. The stabilization energy ($\Delta G° = -15.5$ kcal/mol) differs by ca. 10% from the energy of the most stable structure calculated by the program. However, our experimental data (the results of the minimal sequence experiment, and chemical modification data for full-length and truncated RNA) are more consistent with the structure shown in Figure 4, particularly in the hairpin loop domain.

The hairpin loop domain consists of a 20-bp stem with two mismatches (CA and GG), two bulged uridines, and a large 21-nt loop. Two tails are mostly single-stranded, making only a short 4-bp helix. In the cloned RNA pool, we have also four clones with single mutations of the major sequence; single isolates with G70U or A22G, and two having G70A (Fig. 4).

In order to determine the minimal sequence required for binding to the Zn-column, we performed a 3′ and 5′ boundary experiment (Fig. 5). The pooled results

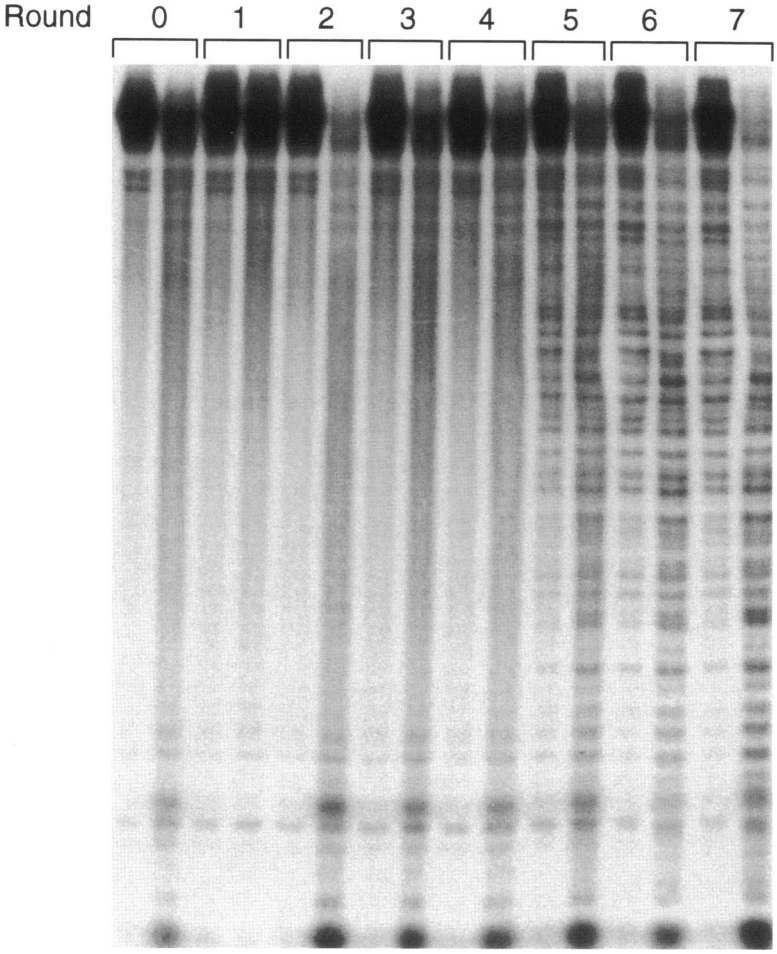

FIGURE 2. Heterogeneity of the selected RNA pools assayed by limited hydrolysis with RNase T1. Internally ^{32}P labeled RNA pools from round 0 to 7 of selection were digested with two different concentrations of RNase T1 and digestion products were electrophoresed through a denaturing 12% polyacrylamide gel.

showed clearly that only the region spanning nucleotides C30 and A72 (the loop and a part of the stem in the secondary structure shown in Fig. 4) was required for binding to the Zn-column.

Hydrolysis of RNA molecules with lead ions has been proven to be a valuable method of probing strong metal ion binding sites (Krzyzosiak et al., 1988; Behlen et al., 1990; Kazakov & Altman, 1991; Ciesiolka et al., 1994) as well as overall RNA conformation (Gornicki et al., 1989; Ciesiolka et al., 1992a, 1992b). Strong specific cleavages induced by Pb ions are thought to occur near strong metal ion binding sites. Therefore, such exceptional cleavages imply that region to be in three-dimensional proximity to the bound ion. However, coordination of the ion may occur via regions distant in the primary structure, as has been shown in yeast $tRNA^{Phe}$ (Brown et al., 1983; Rubin & Sundaralingam, 1983). Moreover, in addition to these strong cleavages near stably bound Pb ions, cleavages of lower intensity preferentially occur in single-stranded RNA regions, whereas helical regions are highly resistant to hydrolysis. Cleavages do occur in double-stranded regions at weak, bulged, or destabilized base pairs. This can be understood because the phosphodiester is not aligned to allow in-line cleavage by 2'-OH in a normal A-form helix. Therefore, helices are resistant and single-stranded RNA regions can also go uncleaved if nucleotides are held out of alignment by stacking or tertiary interactions, but all flexible regions will be cleaved.

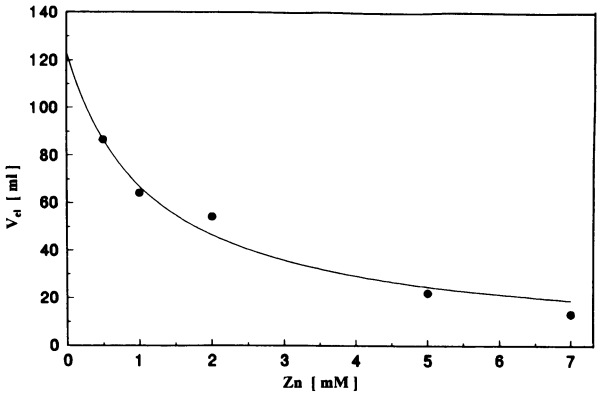

FIGURE 3. Dissociation constant measurements by isocratic affinity elution in the presence of Zn ions. Experimental details are described in the Materials and methods. The line is the least-squares fit to the data, assuming an ideal binding isotherm.

We have applied the lead hydrolysis method to structural analysis of the selected Zn-binding RNA. A

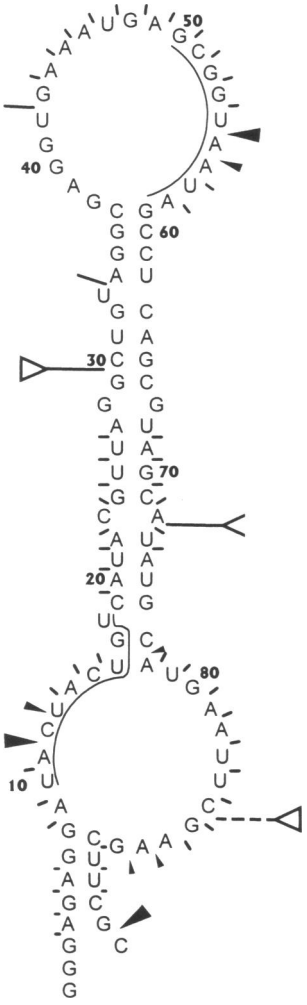

FIGURE 4. Predicted secondary structure of Zn-binding RNA. Boundaries obtained from the 3′ ^{32}P labeled (——◁) and the 5′ ^{32}P labeled (——≺) RNA (see Fig. 5) are indicated. An additional "weaker" boundary observed from the 3′ ^{32}P labeled RNA (- - -◁; see also Fig. 5 B) is caused, most likely, by the association of a small fraction of short RNA fragments with the full-length molecule. Strong (◀■), moderate (—), and weak (–) Pb^{2+} cleavages (see Fig. 6) are also shown. Lines along the sequence mark two regions that might be paired to form a pseudoknot structure.

representative autoradiogram of hydrolysis of 5′-end labeled RNA with Pb ions at concentration 0.25 and 1 mM is shown in Figure 6 and the results are displayed in Figure 4. There are two regions in the molecule strongly cleaved by Pb: close to the 5′-terminus at A11 and C12 and within the loop region at U54 and A55. It seems that both regions are in the vicinity of a bound Pb ion. However, it is not clear whether the cleavages are induced from two independent binding sites or from one site but with the RNA arranged into a pseudoknot structure with the 5′-terminal region folded back over the loop (regions U10–U18 and G50–A58 can be paired with only one CA mismatch).

The distribution of weaker cleavages, in particular, cleavages within the loop region between U42–A58, and the resistance to hydrolysis of the stem regions G28–C37 and G59–G67 with a single cleavage at bulged U33, is consistent with the proposed hairpin loop-like structure for that domain. The region G38–G41, composed of four consecutive purines resistant to hydrolysis, may be strongly stacked. The remaining part of the molecule is much more susceptible to hydrolysis, reflecting either its lower stability (the stem U16–A27/U68–A78 is composed mostly of AU base pairs), or because of conformational heterogeneity in that domain.

Strong, specific cleavages at A11–C12 and U54–A55 induced in the presence of 0.25 mM Pb ions were diminished and finally suppressed when the reaction was performed in the presence of Zn ions at 0.25 and 2 mM (Fig. 6). Cleavages in other regions are much less or not affected in the presence of Zn ions. This suggests that Pb and Zn ions may compete for an overlapping localized binding site. Similar competition experiments in the presence of several other divalent metal ions and their effect on the cleavages induced in the loop region is shown in Figure 6. Local suppression of Pb-induced cleavage was also observed in the presence of Cd, even more strongly with Co and Ni, much weaker with Mn, whereas Ca had almost no effect on lead cleavages. These observations were in good agreement with the results of a parallel column assay. RNA was most strongly retained on the IDA-column charged with Ni and Co, but eluted in the void volume from the column charged with Ca (not shown).

Structure of the Zn-binding domain

Because the boundary experiment suggested that the 5′- and 3′-terminal regions of the selected RNA are superfluous for binding to the Zn-column, we synthesized the truncated molecule in which nucleotides A4–U18 and U79–A87 were deleted. The most stable calculated secondary structure of this smaller RNA ($\Delta G° = -18.3$ kcal/mol) corresponds to the hairpin loop domain of the full-length molecule (the region C19–A78 in Fig. 4) with 5′ and 3′ tails, 5′-GGG-3′ and 5′-AGCUUCGC-3′, respectively. The truncated RNA showed Zn-column affinity similar to the longer original RNA (10% difference in peak position) but the flow-through-fraction (misfolded molecules?) decreased from 15 to 5% of the RNA applied (data not shown).

Lead hydrolysis of the truncated RNA (Fig. 7A) also closely resembles that of the corresponding hairpin loop domain of full-length RNA (Fig. 6) and was consistent with the predicted secondary structure. Thus, the pseudoknot noted above, if it existed, was not crucial for ion affinity, because it is deleted in the truncate.

Hairpin loop structure was also consistent with the results of chemical modification with DEPC (Fig. 7B). This reagent modifies N^7 positions of adenosine residues and is sensitive to stacking interactions (Ehres-

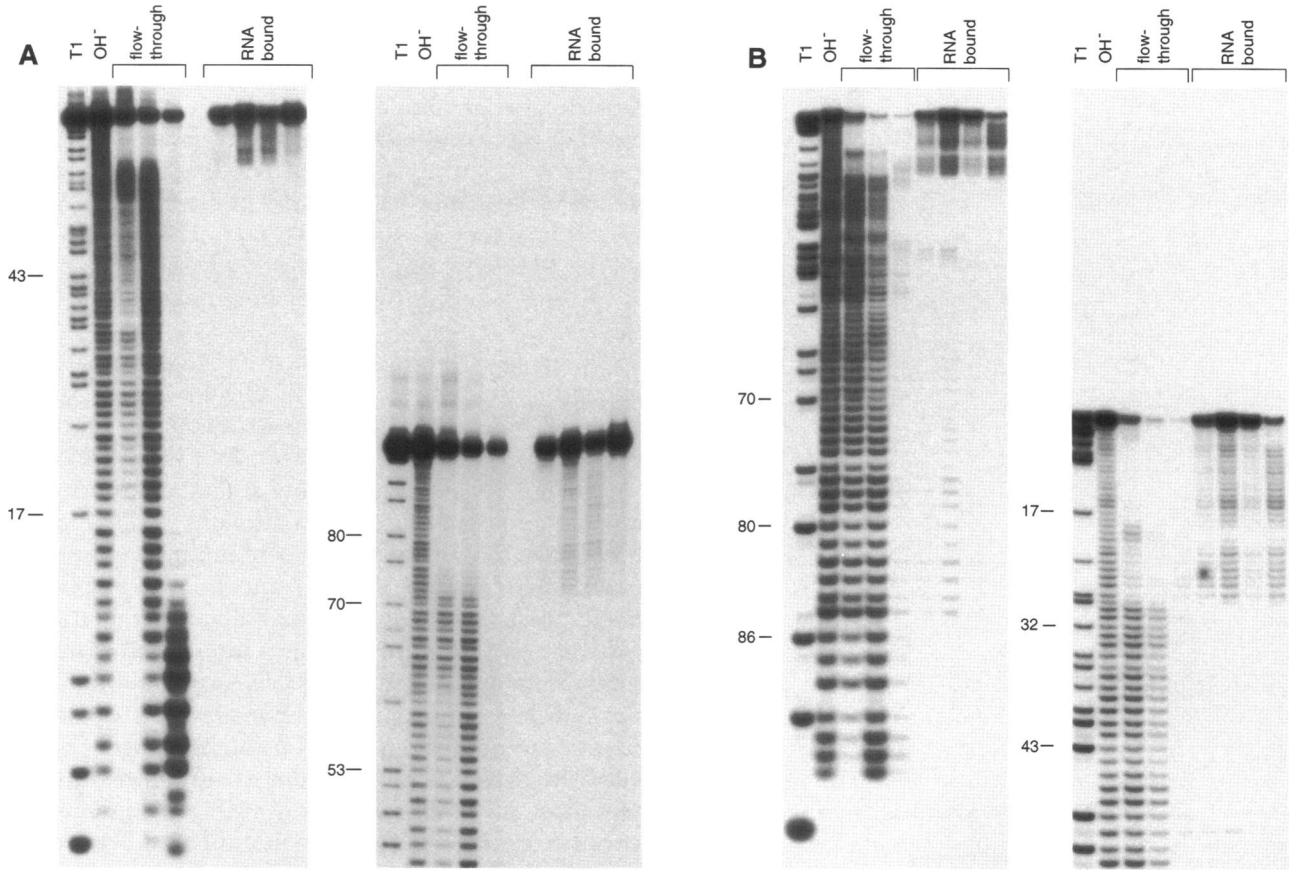

FIGURE 5. Minimal sequence requirement for the binding of the selected RNA to the IDA-Sepharose column charged with Zn ions. RNA was either labeled at its (**A**) 5′-end or (**B**) 3′-end with ^{32}P and partially digested under alkaline conditions. Digestion products were loaded onto the Zn-column, eluted with the start buffer, and subsequently with buffer containing 50 mM EDTA (see Fig. 1B). Seven different fractions were collected: three in the void volume (flow-through), three from the major elution peak, and one eluted with EDTA (RNA bound). RNA from these fractions was recovered by ethanol precipitation and run on a 12% polyacrylamide gel along with OH^-–alkaline hydrolysate and T1–partial RNase T1 digest.

mann et al., 1987). In the truncated RNA, only residues in the loop region (e.g., A39, A44, A45, A46, A49, A55, A56, and A58) and in the single-stranded 3′-terminus (e.g., A78 and A88; numbering according to the full-length RNA) were modified.

Because Zn ions are known to interact with the bases, preferentially with N^7 of guanine (Rubin et al., 1983; Saenger, 1984), we performed chemical protection experiments with DMS and DEPC (Fig. 7B,C). All substantial differences in the chemical reactivity of N^7 atoms in presence of Zn occurred in the loop region of the truncated RNA. In the absence of Zn, all the A's and G's present in the loop were modified. Notably, protections observed in the presence of Zn occurred in the regions G38–G43 and A49–A58 adjoining the double-stranded stem (Fig. 7D). The remaining part of the loop between A44 and G48 was not affected.

Especially remarkable were an unexpected Zn-induced DEPC hyperreactivity of A55 and A56, and an apparently changed base specificity for DMS, which modified the adenosines in 38-GA and 43-GA, leaving the guanosines protected by Zn ions. The results of chemical modification of the full-length RNA in the hairpin loop-like region, as well as protections observed within the loop in the presence of Zn, were identical in the truncate and full-length RNA (data not shown).

Watson–Crick positions were separately probed, using DMS and CMCT reactions assayed with reverse transcription, and are summarized in Figure 8. No significant protection effects were observed in the presence of Zn, although a few changes in the relative intensity of several bands could be reproducibly noted. It seems likely that there are no extensive interactions within the loop that involve Watson–Crick pairing. However, reactivity varies distinctly across the loop, suggesting that the loop has an ordered structure.

In order to get further structural information on the Zn-binding domain, we looked for UV crosslinking. In folded, highly structured RNA molecules, specific, intramolecular crosslinks can often be formed upon irradiation with short-UV light. Irradiation of the 3′- and

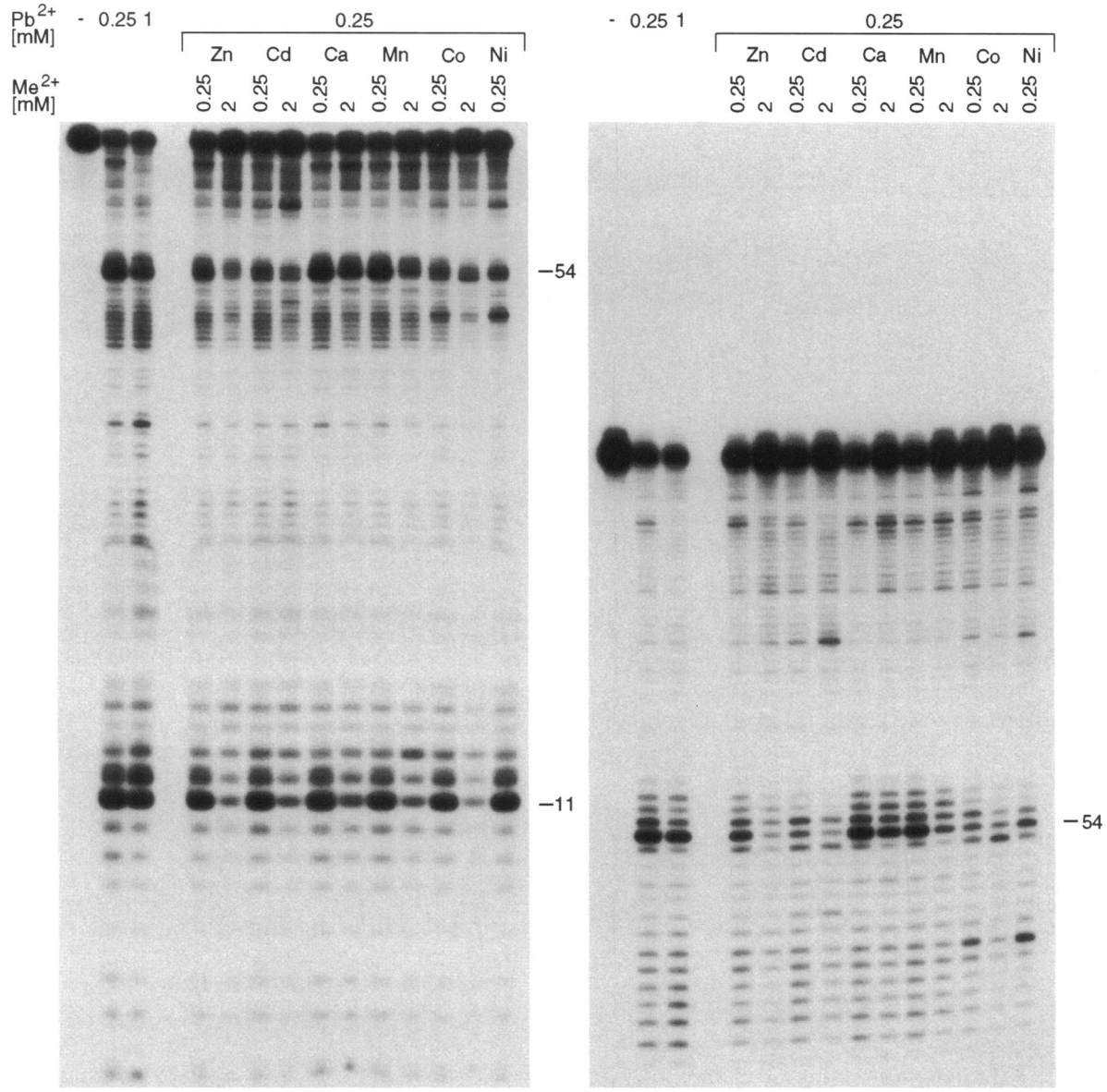

FIGURE 6. The relative abilities of different divalent metal ions to inhibit strong Pb-induced cleavages. The 5′-end ^{32}P-labeled RNA was hydrolyzed with 0.25 mM Pb^{2+} at 23 °C for 20 min in the presence of different divalent ions at 0.25 and 2 mM concentration as indicated. Digestion products were separated on a denaturing 12% polyacrylamide gel.

5′-end labeled Zn-binding RNA in the absence and presence of Zn revealed several photoproducts migrating above the intact RNA on a denaturing polyacrylamide gel (Fig. 9A). The bands of relatively high intensity were observed in region a of the gel both in the absence and presence of Zn. In contrast, region b of the gel contains a strong band that appeared only in the presence of Zn. Six percent of the RNA molecules formed the Zn^{2+}-dependent crosslinking product; this was the major crosslink formed in the presence of Zn^{2+}. The 6% yield is not maximal, but was obtained at the minimum irradiation giving a sufficient yield for characterization. The gel-purified crosslinked RNA species were mapped by partial alkaline hydrolysis of 5′- and 3′-end labeled material (Fig. 9B). RNAs from band b produced ladders with distinct gaps after A39 and starting from A56 for the 5′- and 3′-end labeled RNA, respectively, indicating that the crosslink was formed between G40 and U57. The RNAs isolated from bands a appear heterogeneous; mixtures of photoproducts in which residues from two opposite RNA strands between C15 and U18 and C77 and A81 become crosslinked would be consistent with the data.

DISCUSSION

For selection of Zn-binding RNAs, we have adopted the method of immobilized metal affinity chromatog-

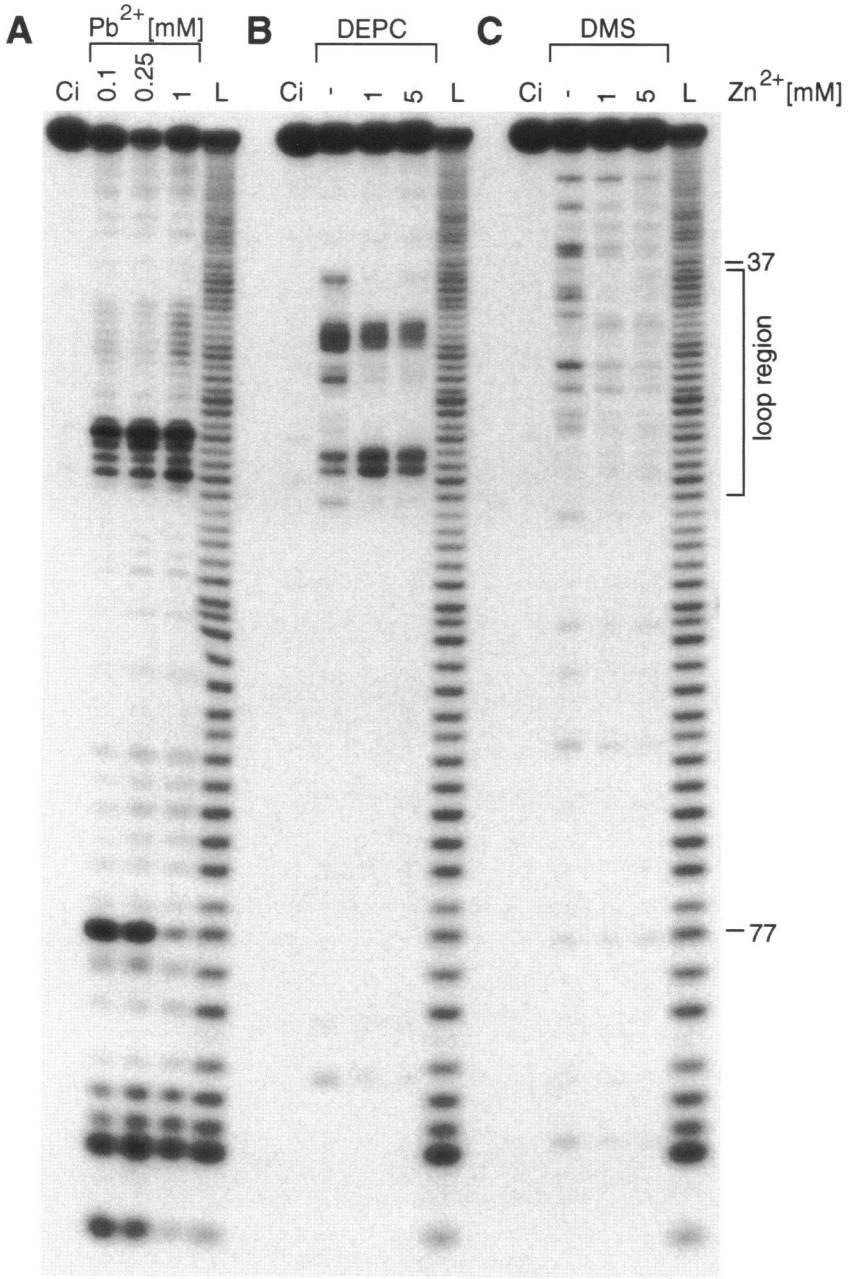

FIGURE 7. Probing of the truncated Zn-binding RNA with (**A**) Pb^{2+}, (**B**) DEPC, and (**C**) DMS. The reactions were performed with 3′-end ^{32}P-labeled RNA at 25 °C for 20 min (Pb and DMS) or 1 h (DEPC). In the reactions with DEPC and DMS, Zn ions at concentration of 1 and 5 mM were also included as indicated and, after the modification, the RNAs were treated with sodium borohydride and aniline (see the Materials and methods). Ci, control lanes, L, alkaline hydrolysate. **D:** Results of DEPC and DMS modification are displayed in the loop region of the RNA structure shown in Figure 4. The dotted line marks a UV-induced crosslink.

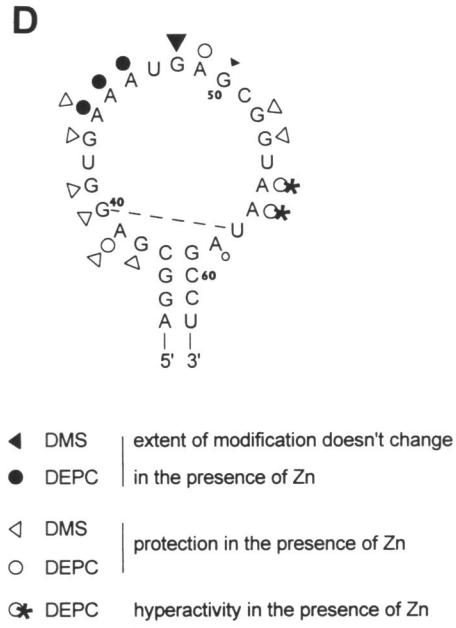

raphy (IMAC), used previously for separation of proteins based on their content of exposed histidine residues (reviewed in Porath, 1992). The method was extremely selective. From the initial RNA pool of $\approx 10^{14}$ 95-mers with 50 nt randomized (20 μg of RNA), seven rounds of selection–amplification isolated a single structure (Fig. 1). The results of competitive affinity chromatography performed at different concentrations of Zn (plus high monovalent and 1 mM Mg ions) suggests K_d of 1.2 ± 0.4 mM for Zn ions (Fig. 3).

The minimal RNA sequence defined in the boundary experiment, the results of lead hydrolysis, and analysis of different secondary structures with similar calculated stabilities are consistent with a hairpin secondary structure for the essential domain (Fig. 4), having a helical stem with bulge defects, and a 21-nt loop.

Isolation of a single large, unique RNA like this is unexpected because of the small size of the ligand, and the many possible ligand atoms (e.g., phosphate oxygens and purine N^7 base atoms) in RNA. A possible explanation is that a relatively large RNA motif is needed to meet selection for binding to the Zn-column. The actual binding site may be small, but its low stability may require imbedding in a larger stable RNA. In addition, the intrinsic constraint of divalent-affinity chromatography, that the RNA must utilize only a subset of coordination positions, may be more stringent than we had originally thought.

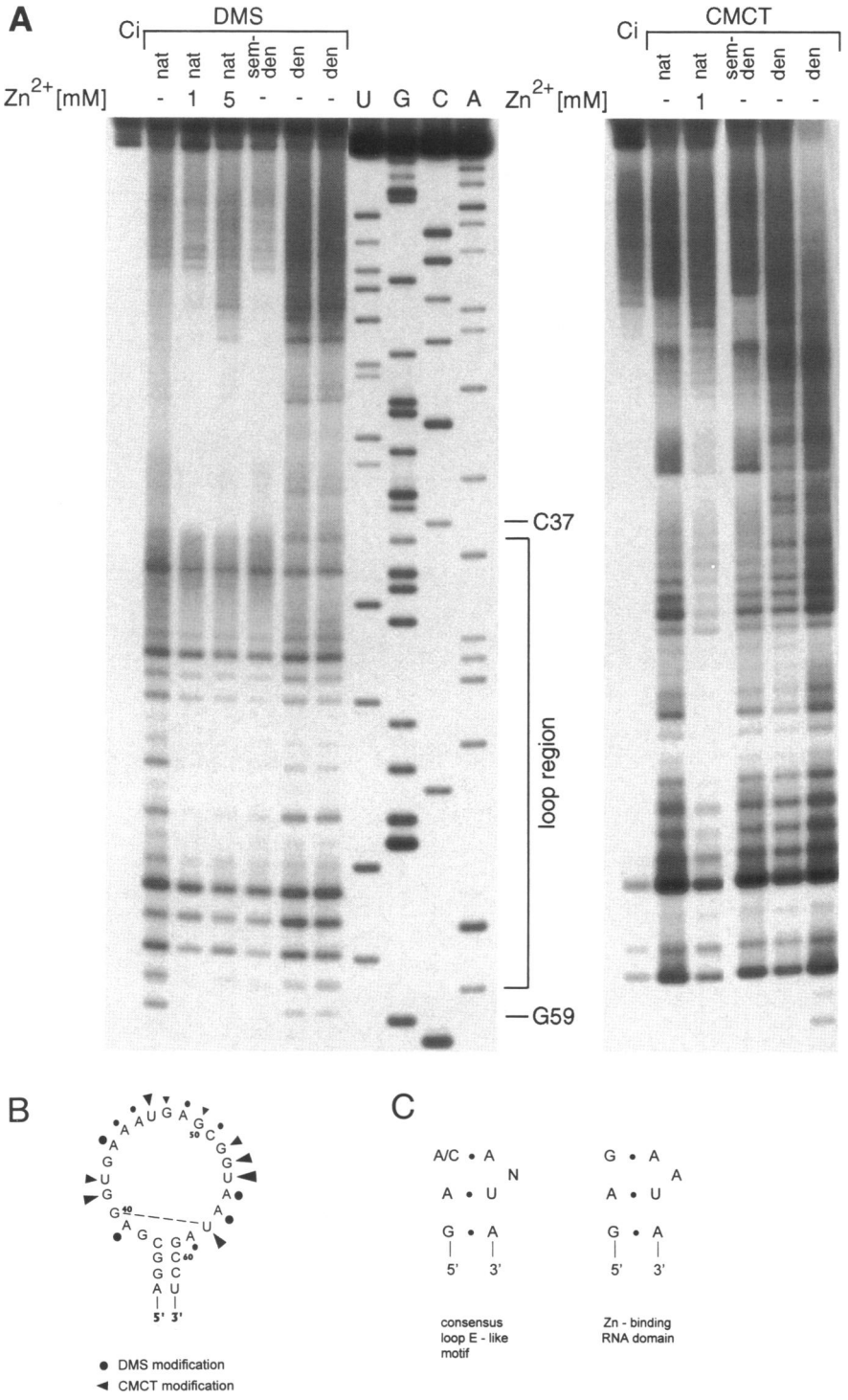

FIGURE 8. Chemical probing of the structure of Zn-binding RNA by alkylation of W-C positions of bases with DMS and CMCT. **A:** DMS and CMCT modification were performed as described in the Materials and methods at 23 °C in native conditions (nat), ± 1 or 5 mM Zn as indicated, and in the presence of 1 mM EDTA at 25 °C (sem-den) or at 90 °C (den). Modification sites were mapped by primer extension with reverse transcriptase using a ^{32}P-labeled 25-mer primer complementary to the 3'-end of the RNA. Reverse transcriptase terminates one base to the 3'-side of the modified nucleotide. A, C, G, U are dideoxy sequencing lanes and lanes Ci are reverse transcription from unmodified RNA. **B:** Summary of the results displayed in the loop region of the RNA structure shown in Figure 4. The dotted line marks a UV-induced crosslink. **C:** The more highly conserved portion of the E-loop motif and the RNA domain of selected Zn-binding RNA are shown.

Within the loop, strong lead-induced cleavages occurred at U54, A55, which are suppressed in the presence of Zn, suggesting that Pb and Zn compete for overlapping binding sites. A similar competition effect occurred also in the presence of Ni, Co, and Cd, whereas in the case of Mn much weaker and Ca almost no effect was observed. By far the simplest interpretation of these results is that a site capable of binding several different divalents in overlapping positions exists in the selected RNA, but a more complex notion that separate sites communicate through structural effects is not formally eliminated. We have provisionally adopted the single-site model.

The RNA specificity for varied divalents is informative. Divalent affinities for sites of simple, somewhat mobile structure usually follow the Irving–Williams affinity series (Frausto da Silva & Williams, 1991): Ca^{2+}, $Mg^{2+} < Mn^{2+} < Co^{2+} < Ni^{2+} < Cu^{2+} > Zn^{2+}$, Cd^{2+}.

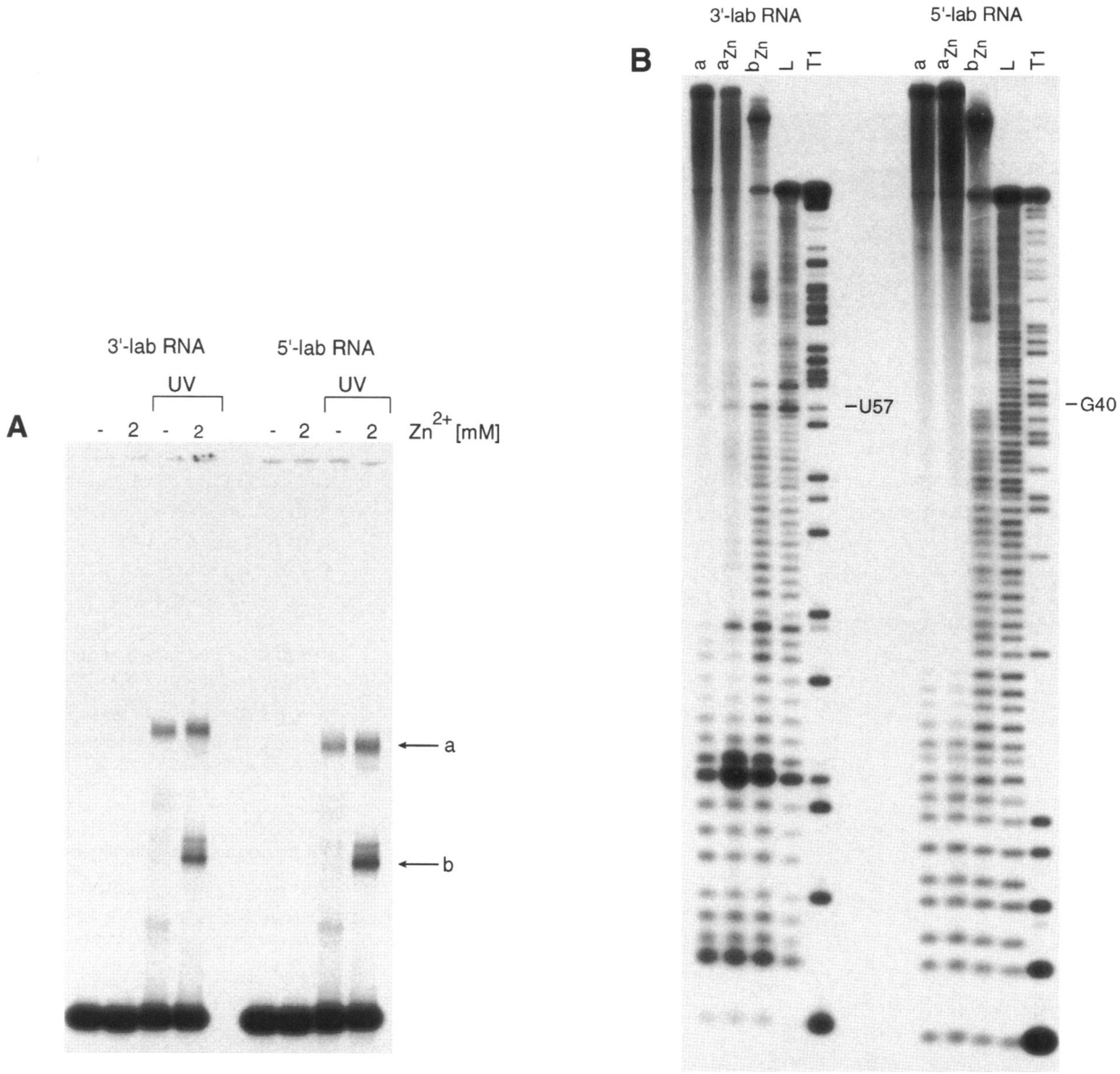

FIGURE 9. UV crosslinking of the Zn-binding RNA. **A:** UV crosslinking of the 5′- and 3′-end labeled RNA (denoted in the figure as 5′-lab RNA and 3′-lab RNA, respectively) performed ± 2 mM Zn ions as indicated. In the control lanes, RNA was not exposed to UV light. **B:** Identification of crosslinked residues in photoproducts a and b isolated from the gel shown in panel A. L, alkaline hydrolysate; T1, RNase T1 digest.

The Irving-Williams series also seems to describe the selected RNA site (Fig. 6). Thus, the selectivity evidence supports a single site for ions, and also suggests that the selected RNA site does not impose strict geometrical or size constraints on the bound ion. This result may therefore be consistent with the evidence for conformational flexibility during binding (Figs. 7, 9), and with the requirement that the RNA contact only a subset of coordination positions, the latter imposed by the affinity selection.

Although a hairpin is required for divalent binding, all nucleotides may not be near the ion. The minimal sequence experiment showed that the region between C30 and A72 was indispensable for Zn-column affinity (Fig. 4). Computerized folding of each progressively shortened molecule suggested that these boundaries might not define the region minimally required for ion-binding per se, but instead the region required for stability of the active stem-loop (not shown).

In order to verify the proposed secondary structure of the Zn-binding domain, we have synthesized a truncated RNA by deleting the regions A4–U18 and U79–A87. The hairpin loop-like structure of this new molecule is now thermodynamically preferred (ΔG = −18.3 kcal/mol). As expected, the smaller RNA showed the important features of the parental molecule: it was bound to the Zn-column with similar affinity and was strongly cleaved by lead in the corresponding re-

gion of the loop. On the other hand, when the 21-nt loop was replaced by a 23-nt random region, only 0.5% of the resulting RNA pool was able to bind to the Zn-column (data not shown). Thus, the sequence of the loop region was indispensable for Zn binding.

The internal structure of the 21-nt loop region is therefore of particular interest. Because Zn ions coordinate preferentially to N^7 nitrogen atoms of guanine residues in nucleosides and polynucleotides (Rubin et al., 1983; Saenger, 1984), we probed the reactivity of N^7 positions of purines ±Zn with DEPC and DMS, in both the full-length RNA and its truncated version. The results showed very clearly that all the Zn-induced protections occurred in the loop region of the RNAs, namely in the regions immediately adjacent to the stem (Fig. 7D). The results of chemical modification of Watson–Crick positions of the bases within the loop of the Zn-binding RNA do not detect definite divalent effects (Fig. 8B), but differential modification can be interpreted as indicating the presence of several nonstandard interactions (see below).

A striking conjunction of divalent effects within the secondary structure suggests the position of the bound divalent ion. Zn^{2+} induces an unusual DMS hyperreactivity of A55 and A56. Opposite these positions, on the other side of the loop, nt 38–41 are protected. These are most easily interpreted as steric and/or electronic effects of a nearby ion. Interestingly, Zn ions also induce the formation of a particular conformer of the loop region in which two nucleotides (G40 and U57) become crosslinked upon irradiation with UV light (Fig. 9). The Zn-dependent crosslink implies that these bases are very close, a few Ångstroms apart, in the Zn^{2+}-bound structure, thereby bringing the two regions that are enhanced/protected together in space. Finally, an ion site here also provides a simple interpretation for the rapid Pb^{2+}-induced cleavages at U54 and A55, which would reflect abstraction of hydrogen from ribose by hydroxide ions bound to a nearby Pb^{2+} (Brown et al., 1983; Rubin & Sundaralingam, 1983). Caution is required because a site distant in the primary structure can stimulate hydrolysis when the backbone passes close to the ion in space, but the coincidence of Zn^{2+}-induced reactivity changes, the crosslink, and the position of Pb^{2+}-stimulated hydrolysis suggests that the divalent site is near the stem-loop junction, within a structure made by pairing the sides of the loop.

Closer examination of the possible arrangements of the loop reveals that simple extension of the stem region by interactions G38A58, A39U57, and G40A55 with bulged A56 resembles the loop E-like motif suggested for a number of functionally important RNA molecules (reviewed in Wimberly, 1994). The highly conserved consensus part of the loop E structure consists of an AG base pair, AU reverse Hoogsteen interaction, a nonconserved bulged nucleotide, and a nonstandard base pair AA or CA (Fig. 8C). An interesting feature of the loop E motif is that, upon irradiation with UV light, the G from the first base pair can be crosslinked to the U from the second reverse Hoogsteen interaction in eukaryotic 5S rRNA and in the viroids (Branch et al., 1985) or, alternatively, to the bulged U in the hairpin ribozyme (Butcher & Burke, 1994). The consensus loop E-like structure and the structure near the Zn site differ in the presence of G instead of A or C in the third base pair and in that particular G is involved in the UV crosslink. Accordingly, we suggest that the Zn-binding structure may be related, but not identical to the loop E motif.

Two virtually identical three-dimensional models of the E-loop motif have been proposed based on NMR studies of RNA oligomers that correspond to the E-loop region of eukaryotic 5S rRNA (Wimberly et al., 1993) and sarcin/ricin stem-loop region of 28S/23S ribosomal RNA (Szewczak et al., 1993). The models rationalize the chemical probing data obtained by others (Romaniuk et al., 1988). Our chemical probing of the loop structure in the region that resembles the highly conserved part of the E-loop motif (Fig. 7D, 8B) agrees well with data obtained for 5S rRNA from *Xenopus laevis* (Romaniuk et al., 1988). The reactivity of A58 (N^7 protected, N^1 modified) is consistent with base pairing with G38, although the proposed geometry for that GA pair (N^7A-N^2G, N^6A-N^3G) in both E-loop models does not explain the resistance of N^7 and N^1 of G38 to chemical modification. However, the corresponding residue was also not modified in 5S rRNA (Romaniuk et al., 1988). As predicted from the reverse Hoogsteen interaction, N^1 of A39 is reactive, but N^7 is not. The reactivity of N^3 position of U57 is not predicted, however. Two adenosine residues, A55 and A56, are the only purine bases in that region whose N^7 positions are highly accessible to modification. Moreover, in the presence of Zn ions, both residues become hyperreactive. A55 and A56 might be isostructural (their N^1 positions are also modified to a very similar extent). One of them is bulged out and corresponds to G75 in 5S rRNA, which is also the only purine residue modified at N^7 position. The second adenosine residue might interact with G40, similar to the interaction G38A58, because accessibility of both pairs to chemical modification is identical. Accordingly, chemical reactivities are consistent with, but do not prove, the existence of a structure related to the E-loop motif. Analogy to the E-loop motif conversely suggests a divalent-binding function for that motif.

Finally, we wish to compare the affinity of the selected site to other RNA molecules. The best characterized is the binding of Mg^{2+} to tRNAs; K_d of the strongest sites is within the range 10–100 μM (for review see Pan et al., 1993). The apparent affinity of ribozymes for divalents can be characterized by K, the concentration of divalent ions required for the reaction to reach half-maximal rate. The hammerhead ribozyme functions

with several divalents (Dahm & Uhlenbeck, 1991), for Mg^{2+}, K is 5.3 mM for cleavage (Perreault et al., 1991) and 13 mM for the ligation reaction (Hertel & Uhlenbeck, 1995), although a 100 μM dissociation constant for free Mg^{2+} was obtained from changes in the RNA CD spectra of the RNA (Koizumi & Ohtsuka, 1991). Mg^{2+}, Sr^{2+}, and Ca^{2+} are capable of supporting the reaction of the hairpin ribozyme with corresponding apparent dissociation constants of 3, 10, and 20 mM (Chowrira et al., 1993). The *Tetrahymena* ribozyme requires Mg^{2+} or Mn^{2+} (about 2 mM) (Cech, 1993) and the ribozyme of ribonuclease P from *Escherichia coli* functions in the presence of $Mg^{2+} \geq 20$ mM, and Mg^{2+} can be replaced by Mn^{2+} or Ca^{2+} (Altman, 1990). Both ribozymes bind specifically several Mg^{2+} ions (Celander & Cech, 1991; Kazakov & Altman, 1991; Christian & Yarus, 1993). The circular form of the *Tetrahymena* pre-rRNA intron in the presence of RNA substrate binds Mg^{2+} with K_d of 2 mM (Sugimoto et al., 1989). In an oligonucleotide model of a group I intron ribozyme substrate resembling the P1 helix, Mn^{2+} binding site was observed with $K_d \geq 0.1$ mM (Allain & Varani, 1995). The ribozyme ribonuclease P from *E. coli* binds three Mg^{2+} ions very tightly ($K_d = 16$ μM) or weakly one Ca^{2+} ion ($K_d = 20$ mM) (Smith & Pace, 1993). However, the formation of the productive intermolecular ribozyme–substrate complex requires a very high concentration of Mg^{2+}, 63 mM, indicating relatively low affinity of Mg^{2+} for the substrate (Perreault & Altman, 1993).

Thus, the apparent affinity of RNA for structurally or catalytically important divalents is heterogeneous, but frequently within the range 10^{-4} to 10^{-2} M. The measured affinity of the selected RNA for Zn^{2+} ($K_d \approx 10^{-3}$ M) is in the middle of this (free energy) range.

We are reselecting Zn affinity, beginning from an RNA pool derived from the truncated Zn-binding RNA, but with the loop replaced by a 23-nt random region. The selection has been altered to allow us, in theory, to select molecules with higher affinity to Zn. The initial RNA pool for reselection, unlike the pool described here, likely contained every possible sequence of 23 ribonucleotides, perhaps also enabling us to perform a phylogenetic analysis and to more completely define possible Zn^{2+} sites in RNA.

MATERIALS AND METHODS

RNA synthesis

The RNA pool with 50-mer random region was generated from a T7 promoter sequence by in vitro transcription (Milligan et al., 1987) of the double-stranded DNA template of the sequence: 5′-GCG AAG CTT CGA ATT CAT GCA TAT G-N_{50}-TGA CAG TAG TAT CCT CTC CC ≪ TAT AGT GAG TCG TAT TAG AGC TCG C-3′, where N is equimolar nucleotides and ≪ is the transcript start.

Selection procedure

A HiTrap Chelating Sepharose (Pharmacia) affinity column (1 mL; capacity ca. 23 μmol divalent/mL gel) was charged with Zn ions by applying 1 mL of 100 mM $ZnCl_2$ solution, washing out excess Zn with 10 mL of distilled water, and equilibrating the column with 5 mL of buffer A: 0.4 M NaCl, 20 mM HEPES-Na, pH 7.0, and 1 mM $MgCl_2$.

Twenty micrograms of internally labeled ^{32}P RNA (4×10^{14} molecules transcribed from 5×10^{13} different DNA templates) in 250 μL of buffer A was heated at 65 °C for 5 min, cooled to room temperature over 15 min, and loaded onto the affinity column. The column was washed with 20 volumes of buffer A and subsequently with the same buffer containing 50 mM EDTA in place of Mg. The EDTA-eluted pool (six column volumes) was passed through small G50 spun columns containing 0.3 M sodium acetate, pH 6.0, the RNA was ethanol precipitated, reverse transcribed, amplified by PCR, and then transcribed into RNA for the next round of selection as described (Tuerk & Gold, 1990).

Determination of K_d

The K_d for binding Zn ions to the RNA in solution (Fig. 3) was determined by isocratic elution (Dunn & Chaiken, 1974; Connell et al., 1993) from the equation: $K_d = L\{(V_{el} - V_n)/(V_e - V_{el})\}$, where L is the free ligand concentration used to isocratically elute RNA loaded onto the affinity column, V_{el} is the median elution volume of RNA eluted in the continuous presence of free ligand, V_e is the median elution volume measured in the absence of free ligand in the column buffer, and V_n is the volume at which an RNA population having no interaction with the column would elute.

Internally labeled RNA (ca. 3×10^5 cpm, 0.125 μM RNA in total volume of 250 μL) was heated at 65 °C for 5 min in buffer A and cooled to room temperature over 15 min. Zn ions were added to an appropriate concentration, samples incubated at room temperature for additional 10 min, and loaded onto the 2-mL Zn-column that had been equilibrated in buffer A containing the same concentration of Zn ions as in the sample.

Heterogeneity of RNA pools—RNase T1 assay

Internally labeled ^{32}P RNAs (ca. 10,000 cpm) from each round of selection were digested with RNase T1 (0.3–1.2 units/2 μg of RNA) in 20 mM sodium citrate, pH 5.0, 1 mM EDTA, 7 M urea buffer, at 55 °C for 15 min. Samples were counted by Cerenkov emission and approximately equalized radioactivities were loaded onto a 12% polyacrylamide, 7 M urea gel.

Minimal sequence requirement for binding to the Zn-column

The RNA was either labeled at the 3′ or 5′ end with ^{32}P, partially hydrolyzed under alkaline conditions (Pan & Uhlenbeck, 1992), and precipitated with ethanol. The digestion products were resuspended in buffer A, subjected to renaturation, and loaded onto the Zn-column. RNA from the collected fractions was precipitated with ethanol, resuspended

in the loading buffer, and loaded onto a denaturing 12% polyacrylamide gel.

Lead hydrolysis

Lead hydrolysis was performed essentially as described (Ciesiolka et al., 1992a, 1992b). Briefly, ^{32}P-end labeled RNA (0.25 μM RNA concentration) was heated at 65 °C for 5 min in the buffer (40 mM NaCl, 20 mM HEPES-Na, pH 7.0, 1 mM $MgCl_2$) and cooled slowly (1 °C/min) to room temperature. In experiments performed in the presence of Zn or other divalent ions, metal ions were added and the samples were incubated at room temperature for 10 min further. Subsequently, lead acetate solution was added and the reactions proceeded at 23 °C for 20 min. The reactions were quenched with EDTA (greater than or equal to twofold excess over divalent ions) in the loading buffer and the samples were analyzed on denaturing 12% polyacrylamide gels.

Chemical modification

For probing N^7 positions of adenine and guanine bases with DMS and DEPC, 3'-end labeled RNA (ca.50,000 cpm, 5 pmol of RNA/200 μL reaction volume) was heated at 65 °C for 5 min in 80 mM HEPES-Na, pH 7.0, 40 mM NaCl, 1 mM $MgCl_2$, and cooled slowly (1 °C/min) to room temperature. Zn ions were added and the samples were incubated at room temperature for 10 min. In the reaction with DMS, 10 μL of the reagent in ethanol (1:12 dilution, v/v) was used for 20 min at 25 °C. Modification with DEPC was performed using 10 μL of DEPC at 25 °C for 1 h. After modification, the RNA was ethanol precipitated and treated with sodium borohydride and aniline as described (Krol & Carbon, 1989). The samples were analyzed on denaturing 12% polyacrylamide gels.

For probing Watson-Crick positions of bases with DMS and CMCT (1-cyclo-hexyl-3-[2-morpholinoethyl] carbodiimide metho-*p*-toluene sulfonate), 1 μg RNA samples were renatured as described above in 80 mM HEPES-Na, pH 7.0, 40 mM NaCl, 1 mM $MgCl_2$ for DMS or 50 mM sodium borate, pH 8.0, 40 mM NaCl, 1 mM $MgCl_2$ for CMCT reaction. The reactions were performed with 10 μL DMS solution (1:12 dilution in ethanol, v/v) or 50 μL CMCT (42 mg/mL in water) at 25 °C for 20 min or in denaturing conditions at 90 °C for 1-2 min. The RNA was precipitated with ethanol and analyzed by primer extension (Krol & Carbon, 1989) with reverse transcriptase and a 24-nt DNA primer complementary to the 3'-terminal region of RNA.

UV-induced crosslinking

^{32}P-end labeled RNA (ca. 3×10^6 cpm, 0.1 μM RNA in total volume of 20 μL) in 80 mM HEPES-Na, pH 7.0, 40 mM NaCl, 1 mM $MgCl_2$ was heated at 65 °C for 5 min and cooled slowly (1 °C/min) to room temperature. Subsequently, Zn ions were added to 2 mM, the samples were incubated at room temperature for 10 min, placed on ice, and irradiated with 254 nm light for 30 min. In the control samples, Zn ions were omitted and/or the samples were not exposed to UV light. After irradiation, RNA was precipitated with ethanol, resuspended in the loading buffer, and loaded onto a denaturing 12% polyacrylamide gel. The crosslinking products and the intact RNA were localized by autoradiography, cut from the gel, and their relative amounts were determined by Cerenkov counting. Crosslinked RNAs were eluted, precipitated with ethanol, and partially hydrolyzed in alkaline conditions (Pan & Uhlenbeck, 1992). The samples were analyzed on denaturing 12% polyacrylamide gels along with partial RNase T1 digests and alkaline ladders of the starting RNA.

ACKNOWLEDGMENTS

We thank USPHS grant GM30881 for support during these experiments. We thank M. Illangasekare for helpful discussions during the initial selections and members of our laboratory for comments on the manuscript.

Received May 18, 1995; returned for revision June 6, 1995; revised manuscript received July 15, 1995

REFERENCES

Allain FHT, Varani G. 1995. Divalent metal ion binding to a conserved wobble pair defining the upstream site of cleavage of group I self-splicing introns. *Nucleic Acids Res 23*:341-350.

Altman S. 1990. Enzymatic cleavage of RNA by RNA. *Angew Chem Int Ed Engl 29*:749-758.

Behlen LS, Sampson JR, DiRenzo AB, Uhlenbeck OC. 1990. Lead-catalyzed cleavage of yeast $tRNA^{Phe}$ mutants. *Biochemistry 29*:2515-2523.

Branch AD, Benenfeld BJ, Robertson HD. 1985. Ultraviolet light-induced crosslinking reveals a unique region of local tertiary structure in potato spindle tuber viroid and HeLa 5S RNA. *Proc Natl Acad Sci USA 82*:6590-6594.

Brown RS, Hingerty BE, Dewan JC, Klug A. 1983. Pb(II)-catalyzed cleavage of the sugar-phosphate backbone of yeast tRNAPhe—Implications for lead toxicity and self-splicing. *Nature 303*:543-546.

Butcher SE, Burke JM. 1994. A photo-crosslinkable tertiary structure motif found in functionally distinct RNA molecules is essential for catalytic function of the hairpin ribozyme. *Biochemistry 33*:992-999.

Cech TR. 1993. Structure and mechanism of the large catalytic RNAs: Group I and group II introns and ribonuclease P. In: Gesteland RF, Atkins JF, eds. *The RNA world*. Cold Spring Harbor, New York: Cold Spring Harbor Laboratory Press. pp 239-269.

Celander DW, Cech TR. 1991. Visualizing the higher order folding of a catalytic RNA molecule. *Science 251*:401-407.

Chowrira BM, Berzal-Herranz A, Burke JM. 1993. Ionic requirements for RNA binding, cleavage, and ligation by the hairpin ribozyme. *Biochemistry 32*:1088-1095.

Christian EL, Yarus M. 1993. Metal coordination sites that contribute to structure and catalysis in the group I intron from *Tetrahymena*. *Biochemistry 32*:4475-4480.

Ciesiolka J, Hardt WD, Schlegl J, Erdmann VA, Hartmann RK. 1994. Lead-ion-induced cleavage of RNase P RNA. *Eur J Biochem 219*: 49-56.

Ciesiolka J, Lorenz S, Erdmann VA. 1992a. Structural analysis of three prokaryotic 5S rRNA species and selected 5S rRNA—Ribosomal-protein complexes by means of Pb(II)-induced hydrolysis. *Eur J Biochem 204*:575-581.

Ciesiolka J, Lorenz S, Erdmann VA. 1992b. Different conformational forms of *Escherichia coli* and rat liver 5S rRNA revealed by Pb(II)-induced hydrolysis. *Eur J Biochem 204*:583-589.

Connell GJ, Illangasekare M, Yarus M. 1993. Three small ribooligonucleotides with specific arginine sites. *Biochemistry 32*:5497-5502.

Connell GJ, Yarus M. 1994. RNAs with dual specificity and dual RNAs with similar specificity. *Science 264*:1137-1141.

Dahm SA, Uhlenbeck OC. 1991. Role of divalent metal ions in the hammerhead RNA cleavage reaction. *Biochemistry 30*:9464-9469.

Davies J, Von Ashen U, Schroeder R. 1993. Antibiotics and the RNA world: A role for low-molecular-weight effectors in biochemical evolution? In: Gesteland RF, Atkins JF, eds. *The RNA world*. Cold

Spring Harbor, New York: Cold Spring Harbor Laboratory Press. pp 185–204.
Dunn BM, Chaiken IM. 1974. Quantitative affinity chromatography. Determination of binding constants by elution with competitive inhibitors. *Proc Natl Acad Sci USA 71*:2382–2385.
Ehresmann C, Baudin F, Mougel M, Romby P, Ebel JP, Ehresmann B. 1987. Probing the structure of RNAs in solution. *Nucleic Acids Res 15*:9109–9128.
Ellington AD, Szostak JW. 1990. In vitro selection of RNA molecules that bind specific ligands. *Nature 346*:818–822.
Famulok M. 1994. Molecular recognition of amino acids by RNA-aptamers: An L-citrulline binding RNA motif and its evolution into an L-arginine binder. *J Am Chem Soc 116*:1698–1706.
Famulok M, Szostak JW. 1992. Stereospecific recognition of tryptophan agarose by in vitro selected RNA. *J Am Chem Soc 114*:3990–3991.
Fersht AR. 1985. *Enzyme structure and mechanism*. New York: W.H. Freeman & Co.
Frausto da Silva JJR, Williams RJP. 1991. *The biological chemistry of the elements*. Oxford: Clarendon Press.
Gornicki P, Baudin F, Romby P, Wiewiorowski M, Krzyzosiak W, Ebel JP, Ehresmann C, Ehresmann B. 1989. Use of lead(II) to probe the structure of large RNA's. Conformation of the 3′ terminal domain of *E. coli* 16S rRNA and its involvement in building the tRNA binding sites. *J Biomol Struct Dyn 6*:971–984.
Hertel KJ, Uhlenbeck OC. 1995. The internal equilibrium of the hammerhead ribozyme reaction. *Biochemistry 34*:1744–1749.
Jenison RD, Gill SC, Pardi A, Polisky B. 1994. High-resolution molecular discrimination by RNA. *Science 263*:1425–1429.
Kazakov S, Altman S. 1991. Site-specific cleavage by metal ion cofactors and inhibitors of M1 RNA, the catalytic subunit of RNase P from *Escherichia coli*. *Proc Natl Acad Sci USA 88*:9193–9197.
Koizumi M, Ohtsuka E. 1991. Effects of phosphorothioate and 2-amino groups in hammerhead ribozymes on cleavage rates and Mg^{2+} binding. *Biochemistry 30*:5145–5150.
Krol A, Carbon P. 1989. A guide for probing native small nuclear RNA and ribonucleoprotein structures. *Methods Enzymol 180*:212–227.
Krzyzosiak WJ, Marciniec T, Wiewiorowski M, Romby P, Ebel JP, Giege R. 1988. Characterization of lead(II)-induced cleavages in tRNAs in solution and effect of the Y-base removal in yeast $tRNA^{Phe}$. *Biochemistry 27*:5771–5777.
Lorsch JR, Szostak JW. 1994. In vitro selection of RNA aptamers specific for cyanocobalamin. *Biochemistry 33*:973–982.
Majerfeld I, Yarus M. 1994. An RNA pocket for an aliphatic hydrophobe. *Nature Struct Biol 1*:287–292.
Milligan J, Groebe D, Witherell G, Uhlenbeck OC. 1987. Oligoribonucleotide synthesis using T7 RNA polymerase and synthetic DNA templates. *Nucleic Acids Res 15*:8783–8798.
Pan T, Long DM, Uhlenbeck OC. 1993. Divalent metal ions in RNA folding and catalysis. In: Gesteland RF, Atkins JF, eds. *The RNA world*. Cold Spring Harbor, New York: Cold Spring Harbor Laboratory Press. pp 271–302.
Pan T, Uhlenbeck OC. 1992. In vitro selection of RNAs that undergo autolytic cleavage with Pb^{2+}. *Biochemistry 31*:3887–3895.
Perreault JP, Altman S. 1993. Pathway of activation by magnesium ions of substrates for the catalytic subunit of RNase P from *Escherichia coli*. *J Mol Biol 230*:750–756.
Perreault JP, Labuda D, Usman N, Yang JH, Cedergren R. 1991. Relationship between 2′-hydroxyls and magnesium binding in the hammerhead RNA domain: A model for ribozyme catalysis. *Biochemistry 30*:4020–4025.
Pley HW, Flaherty KM, McKay DB. 1994. Three-dimensional structure of a hammerhead ribozyme. *Nature 372*:68–74.
Porath J. 1992. Immobilized metal ion affinity chromatography. *Protein Expr Purif 3*:263–281.
Prudent JR, Uno T, Schultz PG. 1994. Expanding the scope of RNA catalysis. *Science 264*:1924–1927.
Romaniuk PJ, Stevenson IL, Ehresmann C, Romby P, Ehresmann B. 1988. A comparison of the solution structures and conformational properties of the somatic and oocyte 5S rRNAs of *Xenopus laevis*. *Nucleic Acids Res 16*:2295–2312.
Rubin JR, Sundaralingam M. 1983. Lead-ion binding and RNA chain hydrolysis in phenylalanine tRNA. *J Biomol Struct Dyn 1*:639–646.
Rubin JR, Wang J, Sundaralingam M. 1983. X-ray diffraction study of the zinc(II) binding sites in yeast phenylalanine transfer RNA. Preferential binding of zinc to guanines in purine-purine sequences. *Biochim Biophys Acta 756*:111–118.
Saenger W. 1984. *Principles of nucleic acids structure*. New York/Berlin/Heidelberg/Tokyo: Springer-Verlag.
Sassanfar M, Szostak JW. 1993. An RNA motif that binds ATP. *Nature 364*:550–553.
Smith D, Pace NR. 1993. Multiple magnesium ions in the ribonuclease P reaction mechanism. *Biochemistry 32*:5273–5381.
Sugimoto N, Tomka M, Kierzek R, Bevilacqua PC, Turner DH. 1989. Effects of substrate structure on the kinetics of circle opening reactions of the self-splicing intervening sequence from *Tetrahymena thermophila*: Evidence for substrate and Mg^{2+} binding interactions. *Nucleic Acids Res 17*:355–371.
Szewczak AA, Moore PB, Chan YL, Wool IG. 1993. The conformation of the sarcin/ricin loop from 28S ribosomal RNA. *Proc Natl Acad Sci USA 90*:9581–9585.
Teeter MM, Quigley GJ, Rich A. 1980. Metal ions and transfer RNA. In: Spiro T, ed. *Nucleic acid–metal ion interactions*. New York: John Wiley & Sons. pp 146–177.
Tuerk C, Gold L. 1990. Systematic evolution of ligands by exponential enrichment: RNA ligands to bacteriophage T4 DNA polymerase. *Science 249*:505–510.
Walsh C. 1977. *Enzymatic reaction mechanisms*. San Francisco: W.H. Freeman & Co.
Wimberly B. 1994. A common RNA loop motif as a docking module and its function in the hammerhead ribozyme. *Nature Struct Biol 1*:820–827.
Wimberly B, Varani G, Tinoco I Jr. 1993. The conformation of loop E of eukaryotic 5S ribosomal RNA. *Biochemistry 32*:1078–1087.
Yarus M. 1993. How many catalytic RNAs? Ions and Cheshire cat conjecture. *FASEB J 7*:31–39.
Zuker M. 1989. On finding all suboptimal foldings of an RNA molecule. *Science 244*:48–52.